

## Racemic $\alpha$ -cyclohexyl-mandelic Acid Resolution across Hollow Fiber Supported Liquid Membrane

D. Huang,<sup>a</sup> K. Huang,<sup>a,\*</sup> S. Chen,<sup>b</sup> S. Liu,<sup>a</sup> and J. Yu<sup>a</sup>

<sup>a</sup>School of Chemistry and Chemical Engineering,  
Central South University, Changsha 410083, China

<sup>b</sup>Key Laboratory of New Material and Technology for Package,  
Hunan University of Technology, Zhuzhou 412008, China

Original scientific paper  
Received: September 30, 2007  
Accepted: September 29, 2008

This paper deals with the resolution of racemic  $\alpha$ -cyclohexyl-mandelic acid containing copper(II) *N*-dodecyl-(L)-hydroxyproline (CuN<sub>2</sub>) as a chiral carrier across hollow fiber supported liquid membrane. A mathematical model of transport and resolution of chiral compounds was deduced, the observed partition coefficient between the feed phase and the membrane phase, the stripping phase and the membrane phase, mass transfer resistance of boundary layer in strip phase inside the hollow fibers, boundary layer in feed phase and mass transfer resistance of the membrane phase are taken into account in the model equations. Using the experimental results, several parameters of the proposed model have been achieved by a nonlinear fitting method. It is a simply mathematical model which can be easily used to predict the concentration of the enantiomers and the separation factor of the resolution process.

*Key words:*

Resolution, hollow fiber supported liquid membrane,  $\alpha$ -cyclohexyl-mandelic acid, model

### Introduction

Over recent years, attention has increased in the use of supported liquid membrane (SLM) as selective separation barriers.<sup>1–3</sup> A SLM achieves resolution through a higher affinity of the liquid membrane for a particular enantiomer, it offers many advantages such as high selectivity, high efficiency of separation, high enrichment efficiency, minimum product contamination, low cost, no phase separation problem, easy scale up option for commercial applications and less use of the organic phase than in the classical solvent extraction process.<sup>4–6</sup> There are three configurations available for a SLM: flat sheet SLM, hollow fiber SLM and spiral wound SLM.

Hollow fiber SLM containing active chiral carriers provide a simple, stable means for studying the transport and selective separation of chiral drugs from dilute aqueous solutions. The most frequent applications of hollow fiber liquid membrane systems for racemic resolution have been in the concentration and selective resolution of chiral amino acids.<sup>7–9</sup> Hollow fiber SLMs are usually prepared by filling the pores of these membranes with the organic liquid composed of the chiral carrier and the diluent. This simple geometry, which is economical for research purposes, uses a very small

amount of organic solution to transport large amounts of drugs.

Optical pure  $\alpha$ -cyclohexyl-mandelic acid (HCHMa) is a kind of important precursor of chiral drugs and can be used to synthesize multiplicate chiral drugs with vital biological activity and well curative effect such as oxybutynin.<sup>10</sup> Chiral extraction for resolution of enantiomers has great potentialities, and it has been highly regarded in recent years.<sup>11–13</sup> So it is necessary to resolute racemic HCHMa into R- and S-enantiomers.

In this work, a hollow fiber supported liquid membrane was used to resolute the racemic HCHMa and a new mathematical model was presented for analyzing the transport of enantiomers. It provides a new way to resolute the racemic HCHMa and a simply mathematical model which can be easily used to simulate and predict the concentration of the enantiomers and the separation factor of the resolution process.

### Theory

In this paper we propose a mechanism for the transport of HCHMa enantiomers through a hollow fiber SLM. Consider a porous carrier-facilitated SLM used for separating R- and S- $\alpha$ -cyclohexyl-mandelic acid of the racemic mixtures. The membrane consists of a chiral carrier dissolved in a water immiscible organic diluent.

\*Corresponding author: Fax: +86-731-8879850;  
E-mail: klhuang@mail.csu.edu.cn

In order to simplify the mathematics and model development, the following assumptions are made: 1. An ideal system exists under complete mixing and constant temperature operation; 2. Constant physical and transport properties; 3. The membrane phase is completely immiscible with the aqueous phase; 4. The volume of the liquid membrane phase is neglected relative to the volume of the feed phase and the strip phase. 5. The observed partition coefficient include (a) partition of the enantiomers and (b) combination of the enantiomers with the carrier.

### Solute partition equilibrium

A mass balance to the hollow fiber module and vessel can be used to determine the change in solute concentration with time:

$$V_f \frac{d\gamma_{fj}}{dt} = -K A_m (\gamma_{fj} - \gamma_{fj}^*) \quad (1)$$

Where  $K$  is the overall mass transfer coefficient,  $V$  represents the aqueous phase volume,  $A_m$  is the membrane transfer area, and  $\gamma$  is the solute mass concentration. The subscripts “j” refers to the enantiomers of the chiral drugs, the subscripts “f” refers to the feed phase (shell side), and the superscript “\*” refers to the solute concentration in the aqueous phase, in equilibrium with the solute concentration in the stripping phase (tube side).

If it is assumed that the solute partition between the two phases is adequately described by a constant observed partition coefficient  $P$  then, integration of eq. (1) and

$$\gamma_{fj}^* = \gamma_{sj} P_{2j} / P_{1j} \quad (2)$$

Eq. (2) indicates the solute concentration in the aqueous phase, in equilibrium with the solute concentration in the stripping phase, and there is an organic membrane phase between these two aqueous phases, so the total partition process includes two processes of  $P_1$  and  $P_2$ .  $P_1$  is observed partition coefficient between the feed phase and the membrane phase,  $P_2$  is observed partition coefficient between the stripping phase and the membrane phase, the observed partition coefficient between these two aqueous phases should be expressed as the ratio of  $P_1$  and  $P_2$ . The subscripts “s” refers to the stripping phase (tube side). The solute concentration in the stripping phase ( $\gamma_{sj}$ ), obtained by mass balance:

$$V_f \gamma_{f0j} + V_s \gamma_{s0j} = V_f \gamma_{fj} + V_s \gamma_{sj} \quad (3)$$

An analytical expression of  $\gamma_{sj}$  versus  $t$  with  $K$  as the unknown parameter can be received as:

$$V_s \frac{d\gamma_{sj}}{dt} = K A_m \left( \gamma_{f0j} + \frac{V_s}{V_f} \gamma_{s0j} - \gamma_{sj} \frac{P_{1j} V_s + P_{2j} V_f}{P_{1j} V_f} \right) \quad (4)$$

### Evaluation of mass transfer correlations

Three individual mass transfer resistances may be considered in hollow fiber resolution process: The boundary layer resistance in the shell side liquid phase; The membrane resistance to solute diffusion across the membrane pores and the boundary layer resistance in the tube side liquid phase. The overall mass transfer resistance, for resolution process using a hollow fiber supported liquid membrane system, can be expressed as:

$$\frac{1}{K_j A_i} = \frac{1}{k_f A_o} + \frac{1}{P_{1j} k_m A_m} + \frac{P_{2j}}{P_{1j} k_s A_i} \quad (5)$$

Where  $k_f$ ,  $k_m$  and  $k_s$  are the individual mass transfer coefficients on the feed phase side, membrane and stripping phase side, respectively, and  $A_i$ ,  $A_o$  and  $A_m$  are the fibers internal, external and logarithmic mean areas, respectively.

$$k_m = \varepsilon D_m / (\delta \tau) \quad (6)$$

$$\tau = 2/\varepsilon - 1 \quad (7)$$

Where  $\delta$ ,  $\varepsilon$ ,  $\tau$  are the thickness of the membrane fibers, porosity of the membrane, tortuosity factor of the membrane pores which takes into account the difference between the effective thickness and the physical thickness.

$D$  is the free bulk diffusion coefficient for the solute calculated using the Wilke-Chang<sup>14</sup> equation:

$$D = 7.4 \cdot 10^{-8} (\varphi M_B)^{0.5} T / (\mu_B V_A^{0.6}) \quad (8)$$

In the present work a Lévêque type equation<sup>15,16</sup> will be used to correlate both the tube side and the shell side mass transfer coefficients:

$$Sh_f = a_f Sc_f^{b_f} Re_f^{c_f} (d_o/L)^{d_f} \quad (9)$$

$$Sh_s = a_s Sc_s^{b_s} Re_s^{c_s} (d_i/L)^{d_s} \quad (10)$$

Where  $Sh$ ,  $Sc$  and  $Re$  are the dimensionless numbers of Sherwood, Schmidt and Reynolds, respectively,  $a$ ,  $b$ ,  $c$  and  $d$  are the unknown parameters. The dimensionless numbers are defined as:

$$Sh = k d / D \quad (11)$$

$$Re = d u \rho / \mu \quad (12)$$

$$Sc = \mu / (\rho D) \quad (13)$$

Where  $k$ ,  $d$ ,  $u$ ,  $\rho$ ,  $\mu$ ,  $D$  are the mass transfer coefficient, dimension, liquid velocity, density, liquid viscosity and diffusion coefficient, respectively.

Integrate eq. (4), the solute concentration in the stripping phase will be expressed as:

$$\gamma_{sj} = \frac{P_{1j}(V_f \gamma_{f0j} + V_s \gamma_{s0j})}{P_{2j}V_f + P_{1j}V_s} + \frac{P_{2j}V_f \gamma_{s0j} - P_{1j}V_f \gamma_{f0j}}{P_{2j}V_f + P_{1j}V_s} \exp\left(-\frac{P_{2j}V_f + P_{1j}V_s}{P_{1j}V_f V_s} A_m K_j t\right) \quad (14)$$

And the expression of separation factor ( $\alpha$ ) can be received as:

$$\alpha = \gamma_{SR} / \gamma_{SS} \quad (15)$$

## Experimental

### Materials

Racemic HCHMa was purchased from Synergetica Changzhou, Ltd. in China. L-hydroxyproline was obtained from Xinghu Biology of Science and Technology Zhaoqing Ltd. in China, the specific optical rotation  $[\alpha]_D^{20} = -85.2^\circ$ , the purity was above 98%. Aldehyde C-12 lauric was purchased from Fluka Chemical Company, the purity was above 97%. Palladium on carbon catalyst was from Shanghai Chemical Reagent Company in China. The polyvinylidene fluoride (PVDF) hollow fiber membrane modules were purchased from Mo-tian Membrane Engineering and Technology Co. Ltd., Tianjin, China.

The PVDF hollow fiber membrane used in this experiment has an effective area of  $A = 0.095 \text{ m}^2$ . The configuration is shown in Table 1.

Table 1 – Characteristics of PVDF hollow fiber membrane

External/Internal diameter	Temperature range	Pore size	PH range	Operating pressure
1.2/0.8 mm	5–45 °C	0.22 $\mu\text{m}$	2–10	$\leq 0.12 \text{ MPa}$

### Analytical method

HPLC was performed with a LC-2010A SHIMADAZU system controller (Kyoto Japan), a sample loop injector of 20  $\mu\text{L}$ , a Shimadzu C-R3A Chromatopac, a Kromasil RP-18, 5  $\mu\text{m}$ , 4.6 mm  $\times$  150 mm column was used for the analysis.

Copper ion concentrations in aqueous phase were determined by volumetric titration with EDTA using 1-(2-pyridyl)azobenzene-2-naphthol (PAN) indicator dye. The copper concentration in the organic phase was determined by first diluting the sample with ethanol and then titrating with EDTA using PAN. HN was synthesized in our lab.<sup>17</sup>

The concentrations of enantiomers in the aqueous were measured by chiral mobile phase HPLC. Chromatographic conditions:<sup>18</sup> concentration of  $\beta$ -cyclodextrin  $c = 9.5 \text{ mmol L}^{-1}$ ,  $V$  [(aqueous  $\text{KH}_2\text{PO}_4$  solution (0.075 mol  $\text{L}^{-1}$ )):  $V$  (ethanol):  $V$  (acetonitrile) = 65:20:15, pH 4.8, flow rate  $Q = 1 \text{ mL min}^{-1}$  and room temperature.

### Resolution of HCHMa

The experiments were carried out on the resolution of racemic HCHMa using copper(II) *N*-dodecyl-(L)-hydroxyproline ( $\text{CuN}_2$ ) as a chiral carrier in a membrane solvent (octanol). The optimal operating conditions were determined by chiral extraction studies detailed in Feipeng and Kelong.<sup>19</sup>  $[\text{Cu}^{2+}] = 5 \text{ mmol L}^{-1}$ ;  $[\text{HN}] = 10 \text{ mmol L}^{-1}$ ;  $[\text{NaAc}] = 0.1 \text{ mol L}^{-1}$ ; pH 4.0. Then, the partition coefficients of S- HCHMa and R- HCHMa are 0.995 and 0.693 respectively. The organic phase was prepared by adding HN (10 mmol  $\text{L}^{-1}$ ) to octanol, and was then contacted with an equal volume of aqueous copper acetate solution ( $\text{Cu}^{2+}$ : 5 mmol  $\text{L}^{-1}$ ) at pH 4.0. The aqueous copper acetate solution was prepared by adding cupric sulfate to acetate buffer. The organic and aqueous solutions were contacted for 48 h. The membrane was soaked in the resulting organic phase for at least 3 h.

The whole solution was immobilized in the pores of the polyvinylidene fluoride polymeric membrane separating two tube- and shell-side aqueous phases. The solution of chiral selectors in the membrane pores was immobilized by pumping the solution of chiral selectors into the tube-side of the hollow fiber membrane module. This solution was circulated for 24 h in order to distribute the dissolved  $\text{CuN}_2$  molecules into the membrane pores.

The feed and strip solutions were prepared by adding perchloric acid to deionized water until the solution pH was 4.0. A racemic mixture of the HCHMa was dissolved in the feed solution (solute concentration: 10 mmol  $\text{L}^{-1}$ ). The feed phase was pumped into the shell-side while the strip solution into the tube-side. At various times, 100  $\mu\text{L}$  samples were removed from the strip solution and the R and S-enantiomers concentrations were determined using HPLC.

## Results and discussions

### Experimental result of enantiomers concentration and separation factor

The experimental data of the enantiomers dimensionless concentration and separation factor of resolution process are shown by dot in Figs. 1 and 2. It can be seen that both enantiomer concen-

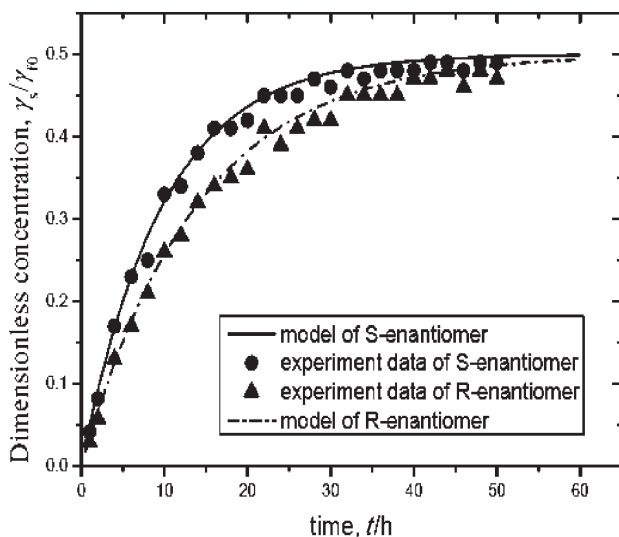


Fig. 1 – Dimensionless concentration profiles of enantiomers in the stripping phase. ● and ▲ experimental data; Solid line: model prediction of dimensionless concentration of the S-enantiomer; Dot line: model simulation of dimensionless concentration of the R-enantiomer.

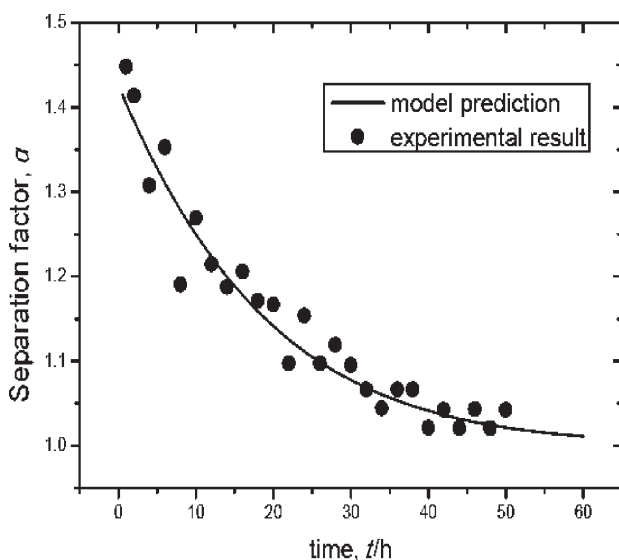


Fig. 2. – Separation factor of the enantioseparation process. ● experimental data of separation factor; Solid line: results computed by eq. (15).

trations of the strip solution increase rapidly in the first few hours, and the S- HCHMa concentration is higher than that of the R- HCHMa. The slope of S- HCHMa is steeper than the slope for R- HCHMa. It is because that the total mass transfer impetus is the highest one at the beginning since that the partition process is far from the equilibrium, and the mass transfer impetus of the S- HCHMa is higher than that of the R- HCHMa because that the observed partition coefficient of the S- HCHMa is higher than that of the R- HCHMa. The concentration difference between the S- and the R- HCHMa in the strip solution shows a maximum. This maximum

concentration difference is determined by the ratio of the observed partition coefficients of the two enantiomers. In this case, the maximum is shown at the time of 20 h. This result can be used as a guideline to determine the optimum operation conditions for the resolution process.

#### Model simulation of enantiomers concentration profiles

There are eight unknown constants of  $a$ ,  $b$ ,  $c$  and  $d$  in the stripping phase and feed phase. According to the research of many workers,<sup>20–22</sup> there are some semi-experiential formulas about the eqs. (10) and (11), and some constants of them are the same:

$$b_f = b_s = 0.33, \quad d_s = 0.33, \quad d_f = 1 \quad (16)$$

Then integrating eq. (5) to eq. (13), the overall mass transfer coefficient will be expressed as a function of four unknown parameters:  $a_f$ ,  $a_s$ ,  $c_f$  and  $c_s$ :

$$\frac{1}{K_j} = \frac{A_i/A_o}{a_f \left( \frac{d u \rho}{\mu} \right)^{c_f} \left( \frac{D_f^2 \mu}{\rho L^3} \right)^{0.33}} + \frac{A_i/A_m}{P_{1j} \left( \frac{\varepsilon D_m}{\delta \tau} \right)} + \frac{P_{2j}/P_{1j}}{a_s \left( \frac{d u \rho}{\mu} \right)^{c_s} \left( \frac{D_s^2 \mu}{\rho L d^2} \right)^{0.33}} \quad (17)$$

Using the experimental data of concentration and separation factor which are shown in Figs. 1 and 2, the four unknown parameters can be obtained by nonlinear fitting method as:

$$a_f = 4.39, \quad a_s = 1.27, \quad c_f = 2.35, \quad c_s = 0.33 \quad (18)$$

The simulation curves of the enantiomers dimensionless concentration are shown by line in Fig. 1, and the correlation coefficients of curve simulation of S-enantiomer concentration and R-enantiomer concentration are 0.996.

#### Model prediction and experimental result of separation factor

Substituting the parameters obtained by nonlinear fitting method into eqs. (14) and (15), the mathematical model of separation factor can be obtained.

Fig. 2 shows the experimental result and model prediction of the separation factor of resolution process. It can be seen that the computational results of separation factor are shown by a solid line which is in good agreement with the experimental data. Therefore, it can be concluded that the parameters

achieved in eq. (18) can be used to calculate the separation factor of this resolution process. It also indicated that the initial separation factor is the highest one achieved during the run, and it declines rapidly in the first few hours, then it approaches to the value of 1 as time passes. According to the eq. (15), the initial separation factor is defined as:

$$\lim_{\tau \rightarrow 0} a = \frac{K_R}{K_S} \quad (19)$$

It means that the ratio of the overall mass transfer coefficient for the S- and R- enantiomer may be used to predict the maximum degree of separation that could be expected under ideal conditions. For this case, the initial separation is calculated to be 1.45.

## Conclusions

Resolution of racemic  $\alpha$ -cyclohexyl-mandelic acid containing copper(II) *N*-dodecyl-(L)-hydroxyproline ( $\text{CuN}_2$ ) as a chiral carrier across hollow fiber supported liquid membrane was carried out successfully.

A mathematical model was developed to analyze the mass transfer and the separation factor. The observed partition coefficient between the feed phase and the membrane phase, the stripping phase and the membrane phase, mass transfer resistance of boundary layer in strip phase inside the hollow fibers, boundary layer in feed phase and mass transfer resistance of the membrane phase were taken into account in the model equations.

Using the experimental results of the enantiomers concentration, several parameters of the proposed model had been achieved by a nonlinear fitting method. The mathematical model was used to predict the separation factor of the resolution process and the computational results of separation factor were in good agreement with the experimental data. It is a simple mathematical model which can be used to predict the concentration and the separation factor of the resolution process.

## ACKNOWLEDGEMENTS

*This work was supported by the National Nature Science Foundation of China (No.20576142)*

## Nomenclature

- A* – area,  $\text{cm}^2$   
*c* – enantiomer concentration,  $\text{mmol L}^{-1}$   
*d* – diameter of the hollow fiber, mm  
*D* – diffusion coefficient,  $\text{cm}^2 \text{s}^{-1}$

- k* – mass transfer coefficient,  $\text{cm s}^{-1}$   
*K* – overall mass transfer coefficient,  $\text{cm s}^{-1}$   
*L* – length of the fiber, cm  
*P* – observed partition coefficient  
*Q* – volume flow rate,  $\text{mL min}^{-1}$   
*Re* – Reynolds number  
*Sc* – Schmidt number  
*Sh* – Sherwood number  
*t* – time, h  
*u* – liquid velocity,  $\text{cm s}^{-1}$   
*V* – volume of aqueous phase,  $\text{cm}^3$

## Greek letters

- $\alpha$  – separation factor  
 $\gamma$  – solute mass concentration,  $\text{mg cm}^{-3}$   
 $\rho$  – density,  $\text{g mL}^{-1}$   
 $\mu$  – liquid viscosity, cP  
 $\delta$  – membrane thickness, cm  
 $\varepsilon$  – porosity of the membrane  
 $\tau$  – tortuosity of the membrane pores

## Subscripts

- f* – denotes feed phase  
*i* – tube side of the hollow fiber  
*j* – enantiomeric form  
*m* – membrane  
*o* – shell side of the hollow fiber contactor  
*R* – R-enantiomer of the racemic mixture  
*S* – S-enantiomer of the racemic mixture  
*s* – denotes stripping phase

## References

1. *Ata, O. N.*, *Chem. Biochem. Eng. Q.* **19** (2005) 25.
2. *Maximini, A., Chmiel, H., Holdik, H., Maier, M. W., J. Membr. Sci.* **276** (2006) 221.
3. *Stankovic, V.*, *Chem. Biochem. Eng. Q.* **21** (2007) 33.
4. *Qian Yang, Tai-shung Chung, J. Membr. Sci.* **294** (2007) 127.
5. *Ueberfeld, J., Parthasarathy, N., Zbinden, H., Gisin, N., Buffle, J.*, *Analytical Chemistry* **74** (2002) 664.
6. *Van de Voorde, I., Pinoy, L., De Ketelaere, R. F.*, *J. Membr. Sci.* **234** (2004) 11.
7. *Hadik, P., Szabó, L.-P., Nagy, E., Farkas, Zs.*, *J. Membr. Sci.* **251** (2005) 223.
8. *Clark, J. D., Han, B. B., Bhowan, A. S., Wickramasinghe, S. R.*, *Sep. Purif. Technol.* **42** (2005) 201.
9. *Hadik, P., Kotsis, L., Eniszné-Bódogh, M., Szabó, L. P., Nagy, E.*, *Sep. Purif. Technol.* **41** (2005) 299.
10. *Prelog, V., Stojanac, Ž., Kovačević, K.*, *Helv. Chim. Acta* **65** (1982) 377.
11. *Zhongzhe, C., Shuihong, C.*, *Journal Chemical Industry and Engineering (China)* **51** (2000) 418.
12. *Prelog, V., Kovačević, M., Egli, M.*, *Angew. Chem.* **28** (1989) 1147.

13. Jérôme, L., Catherine, G. G., Sonya, T. H., Jonathan, J. J., *Angew. Chem.* **39** (2000) 3695.
14. Reid, R. C., Prausnitz, J. M., Sherwood, T. K., *The properties of Gases and Liquids*, 3rd edn., McGraw-Hill, New York, 1977.
15. Dahuron, L., Cussler, E. L., *AIChE J.* **34** (1988) 130.
16. Prasad, R., Sirkar, K. K., *AIChE J.* **34** (1988) 177.
17. Ding, H. B., Carr, P. W., Cussler, E. L., *AIChE J.* **38** (1992) 1493.
18. Shanshan, H., Yizu, W., Meiren, Sh., *Fine Chemical.* **21** (2004) 731.
19. Feipeng, J., Kelong, H., Xia, Y., Xuehui, Zh., Jingang, Y., *J. Bio. Sci.* **9** (2006) 1149.
20. Ortiz, I., Galan, B., Roman, F. S., Ibanez, R., *AIChE J.* **47** (2001) 895.
21. Gawronski, R., Wrzesinska, B., *J. Membr. Sci.* **168** (2000) 213.
22. Wu, J., Chen, V., *J. Membr. Sci.* **172** (2000) 59.